Proceedings of 2004 IEEE/RSJ International Conference on
Intelligent Robots and Systems
September 28 - October 2, 2004, Sendai, Japan

Advanced Sonar and Laser Range Finder Fusion for Simultaneous Localization and Mapping

Albert Diosi and Lindsay Kleeman
ARC Centre for Perceptive and Intelligent Machines in Complex Environments
Department of Electrical and Computer Systems Engineering
Monash University, Victoria 3800, Australia
Email: {Albert.Diosi;Lindsay.Kleeman}@eng.monash.edu.au

Abstract— **Increasing the information content of measurements can ease some of the problems associated with simultaneous localization and mapping (SLAM). We present an approach for combining measurements from a laser range finder with measurements from an advanced sonar array capable of accurate range and bearing measurements and edge, corner and plane classification. In our approach sonar aids laser segmentation, laser aids good sonar point feature selection and laser and sonar measurements of the same object are fused. We also present a novel approach for fitting right angle corners to laser range data, which enables simple error estimation through the minimization of sum of square range residuals. The results are then used for SLAM with a mobile robot.**

I. Introduction

Mobile robots that build their own maps whilst using them for localization represent an important step towards creating useful autonomous mobile robots. There has been a large variety of sensors used while performing simultaneous localization and mapping (SLAM): sonar (measuring only range) [9], advanced sonar measuring range and bearing to planes corners and edges [4][17], laser range finders [12], monocular vision [19] and stereo vision [5]. Often a combination of sensors is used to improve performance such as vision with laser [3].

There are several reasons for sensor fusion. When different sensors are measuring the same percept, false negatives can be rejected and measurement precision can be improved. In case of complementary sensing, each sensor measures a different percept which complement each other. For example in [1] vertical lines from a camera are used together with horizontal line segments from a laser range finder for localization. It was found that on long corridors which have few horizontal line features that aid localization along the corridor, the use of vertical lines improved localization performance dramatically.

In general, the motivation behind fusion of laser and sonar lies in their complementary character. The main drawbacks of simple sonar systems are specularity, wide beam width and crosstalk [13]. Smooth walls act like mirrors [15], making only walls with $\approx 90^\circ$ angle to the acoustic beam detectable. Objects having good sound insulating properties might not appear in the measurements at all. Planar laser scanners on the other hand, can miss obstacles which are not in their sensing plane. The detection of mirrors and glass doors can be a problem as well.

Fusion of laser and sonar has been done for different purposes. In [13] sonar and laser readings were combined into a sector map for obstacle avoidance. Point features extracted from sonar readings which were recorded at different positions are used for localization in [12] together with line segments and door features from a laser range finder. Fusion of sonar and laser measurements took place in a Kalman filter when updating the estimated robot location with the measurements of landmarks.

When mapping, laser measurements can be used to filter out spurious sonar measurements [13][21][7] or vice versa [15]. Then measurements can be stored in an occupancy map [21][8], or features such as lines and corners can be extracted and combined as in [7]. Alternatively, belief in the existence of line features stemming from laser measurements can be reinforced using sonar measurements as in [15]. Line features can also be extracted from an occupancy map generated using both sensing modalities [13]. Not all of these referenced papers use simple sonar sensors capable of measuring range only. In [21] a special "triaural" sensor was used, which could measure range and bearing to corners, planes and edges. However much of this extra information was wasted by representing the measurements with an occupancy grid.

Features used in SLAM range from raw laser scan points [20] to point features representing trees [18]. Line segments and corners are often used as features. Their extraction from laser scans can be simple, and they provide robust protection against the accidental inclusion of artefacts from moving objects such as humans. Corner features, if their orientation is known, have the advantage that their re-observation can completely determine a robots pose. Fitting a corner to points representing a right angle corner can be done by minimizing the square sum of perpendicular distances of points from two orthogonal lines as in [11], essentially by solving a constrained least squares problem. However when results are to be used in a Kalman filter, an accurate error model of the corner estimate is also necessary.

The term advanced sonar [16] used in this paper refers to sonar that measures range and bearing accurately - typically to 0.2 mm and 0.1 degrees at 3 metres range when the speed of sound is calibrated. The advanced sonar is also capable of classifying targets into right angled concave corners, planes and point/edge features - all in a single

0-7803-8463-6/04/$20.00 ©2004 IEEE

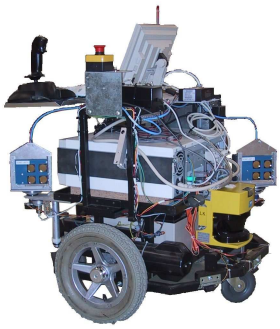

Fig. 1. SLAMbot, the testbed for our mapping experiments.

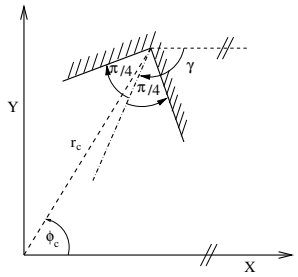

Fig. 2. Meaning of corner parameters.

measurement cycle. By using a transmitted double pulse sequence that is easily identified, interference from other sonar sensor is rejected.

This paper presents new results of simultaneous localization and mapping using advanced sonar and laser range measurements. The advanced sonar aids laser line segmentation by detecting small edge and corner features not seen by the laser due to the larger range quantization and error of the laser. For example doors that are not flush with a corridor are often merged with the corridor line segment with laser alone, however doorjambs are easily detectable to the advanced sonar as edges and small corner features, thus providing a cue for line segmentation in laser measurements. Planes and corners measured by laser and sonar are fused, achieving greater robustness and accuracy. Typically the advanced sonar range and bearing measurements are more accurate within a 5 metre range, whilst laser provides measurements along a line segment rather than just at the normal point as is the case for sonar. The paper also presents a novel approach to fitting right angle corners to range data in polar coordinates that enables simple error estimation essential for a Kalman filter fusion process.

II. Hardware Description and Low Level Processing

The testbed for our experiments is a differential drive robot called SLAMbot (see fig. 1). It is equipped with odometry, 2 advanced sonar arrays on panning mechanisms, and a Sick PLS laser range finder.

A. Odometry

Mounted on each of SLAMbots driving wheels are optical encoders with a resolutions of 2000 steps per revolution that are sampled every 10 ms. The following equations describe the state of odometry $\mathbf{x} = [x\ y\ \theta]^T$:

$$x_{k+1} = x_k - \frac{L_r + L_l}{2}\sin(\theta_k + \frac{L_r - L_l}{2D}) \quad (1)$$

$$y_{k+1} = y_k + \frac{L_r + L_l}{2}\cos(\theta_k + \frac{L_r - L_l}{2D}) \quad (2)$$

$$\theta_{k+1} = \theta_k + \frac{L_r - L_l}{D} \quad (3)$$

where L_r, L_l are distances traveled by the right and left wheel and D denotes the wheelbase. In our error model as in [16], we have assumed, that the sources of odometry errors are random white nose added to the wheel separation and to distances traveled by the wheels. We have propagated the odometry covariance matrix P_k in the conventional way:

$$\mathbf{P_{k+1}} = \frac{\partial \mathbf{x}_{k+1}}{\partial \mathbf{x}_k}\mathbf{P_k}\left(\frac{\partial \mathbf{x}_{k+1}}{\partial \mathbf{x}_k}\right)^T + \frac{\partial \mathbf{x}_{k+1}}{\partial \mathbf{u}_{k+1}}\mathbf{Q_{k+1}}\left(\frac{\partial \mathbf{x}_{k+1}}{\partial \mathbf{u}_{k+1}}\right)^T \quad (4)$$

where $\mathbf{u_{k+1}} = [L_r\ L_l\ D]^T$, and

$$\mathbf{Q_{k+1}} = \begin{bmatrix} K_R^2 L_r^2 & 0 & 0 \\ 0 & K_L^2 L_l^2 & 0 \\ 0 & 0 & K_D^2 D^2 \end{bmatrix} \quad (5)$$

K_R, K_L, K_D are model parameters chosen empirically.

B. Advanced Sonar Array

The advanced sonar sensors mounted on the robot are capable of measuring the range and bearing of planes, right angle corners and edges with $\sigma_{bearing} \approx 0.1^\circ$ and $\sigma_{range} \approx 0.2\ mm$ [16]. They are mounted on panning mechanisms which are swept back and forth continuously. The sonar sensors classify reflectors into planes, corners and edges. Small right angled reflectors formed from 1 cm moldings on the walls of the corridors are classified as edge reflectors.

The error model adopted for the sonar sensors is derived simply from random white Gaussian noise added to bearing measurements and to the speed of sound. The standard deviations of these errors are taken as 2° for bearing and 2% of the speed of sound and were chosen to account for changes in air temperature, air turbulence, unmodelled robot vibrations and association errors.

C. Sick PLS Laser Range Finder

The Sick PLS is a time-of-flight laser range finder that scans in a horizontal plane with 0.5° resolution in the bearings and $5\ cm$ resolution in the range. In [6] a detailed range error model can be found that was applied to line segment systematic and random error modeling. A novel approach to line fitting in polar coordinates is also presented there which minimizes range residuals. These results are used in this work for line fitting and error modeling. A simple treatment of systematic error estimates is to increase the estimated line covariance matrices by adding squared systematic errors to diagonal elements of the covariance matrices. This error estimate becomes optimistic when the

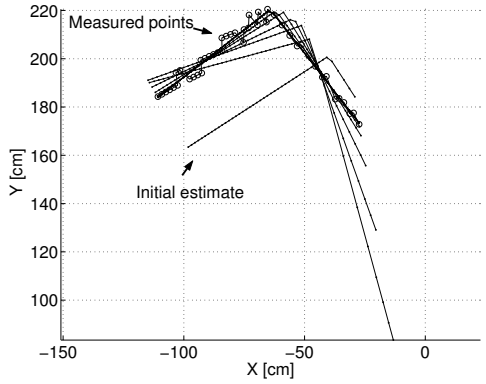

Fig. 3. Corner estimation depicted in Cartesian coordinates.

same feature is observed repeatedly, since the systematic errors are of course correlated, rather than independent as implicitly assumed by the error model.

For fusion of right angle corners, a corner fitting method is necessary. In [11] a method for fitting orthogonal lines is described, where the association of points to lines is assumed to be known. A singular value decomposition is applied to minimize the sum of square distances of the points from the fitted straight line. Since the laser scanner operates fundamentally in polar coordinates by measuring ranges to objects at discrete bearings, the errors in Cartesian coordinates are correlated. Moreover, the covariance matrix of each point is different, which makes an accurate error estimation for the method described in [11] complicated. To make the error estimation simpler and more accurately model the fundamental range error mechanism, we have developed a corner fitting approach which minimizes the square sum of range residuals.

As can be seen from fig. 2 we describe a right angle corner with the range r_c and bearing ϕ_c of its centre and the angle γ of its bisecting line with the X axis. Then the angles of the normals of the lines constituting the corner are $\gamma+\frac{\pi}{4}$ and $\gamma-\frac{\pi}{4}$. The lines themselves can be described with the equation of a line in polar coordinates:

$$d = r\cos(\gamma \pm \frac{\pi}{4} - \phi) \tag{6}$$

where ϕ is the bearing of range reading r and d is the distance of the line from the origin. Since both lines go through (ϕ_c, r_c), (6) can be written as:

$$d = r_c\cos(\gamma + sign(\phi_i - \phi_c)\frac{\pi}{4} - \phi_c) \tag{7}$$

where to distinguish between the lines, we have used the fact that the measured laser bearings ϕ_i belonging to the first line are smaller than ϕ_c, and bearings belonging to the second line are bigger than ϕ_c. Then measured ranges can be modeled as:

$$r_i = \frac{d}{\cos(\gamma + sign(\phi_i - \phi_c)\frac{\pi}{4} - \phi_i)} = \\ = \frac{r_c\cos(\gamma + sign(\phi_i - \phi_c)\frac{\pi}{4} - \phi_c)}{\cos(\gamma + sign(\phi_i - \phi_c)\frac{\pi}{4} - \phi_i)} \tag{8}$$

Using linear regression iteratively on the linearized version of (8):

$$r_i - r_{0i} \approx \frac{\partial r_i}{\partial \phi_c}\Delta\phi_c + \frac{\partial r_i}{\partial r_c}\Delta r_c + \frac{\partial r_i}{\partial \gamma}\Delta\gamma \tag{9}$$

where

$$\frac{\partial r_i}{\partial \phi_c} = \frac{r_{c0}\sin(\gamma_0 + sign(\phi_i - \phi_{c0})\frac{\pi}{4} - \phi_{c0})}{\cos(\gamma_0 + sign(\phi_i - \phi_{c0})\frac{\pi}{4} - \phi_i)} \tag{10}$$

$$\frac{\partial r_i}{\partial r_c} = 1 \tag{11}$$

$$\frac{\partial r_i}{\partial \gamma} = \frac{r_{c0}\sin(\phi_{c0} - \phi_i)}{\cos^2(\gamma_0 + sign(\phi_i - \phi_{c0}) - \phi_i)}, \tag{12}$$

can provide an estimate on the corner parameters. Equation 9 can be restated in vector form as

$$\mathbf{\Delta r} = \mathbf{r_m} - \mathbf{r_0} = \mathbf{H_0}\mathbf{\Delta b} + \mathbf{R} \tag{13}$$

Where

$$\mathbf{H_0} = \begin{bmatrix} \cdots & \cdots & \cdots \\ \frac{\partial r_i}{\partial \phi_c} & \frac{\partial r_i}{\partial r_c} & \frac{\partial r_i}{\partial \gamma} \\ \cdots & \cdots & \cdots \end{bmatrix} \tag{14}$$

$$\mathbf{\Delta b} = [\Delta\phi_c \quad \Delta r_c \quad \Delta\gamma]^T \tag{15}$$

$\mathbf{R}$ is a vector of measurement noise with a covariance matrix $\sigma_r^2 I$ and $\mathbf{r_m}$ is a vector containing measured ranges.

Using linear regression [22] iteratively on the linearized problem (9), we can find (ϕ_c, r_c, γ) which minimizes the square sum of range residuals, the following way:

$$\mathbf{r_j} = [r_{j1} \ \ldots \ r_{ji} \ \ldots \ r_{jn}]^T = \\ = \left[\ldots \ \frac{r_{cj}\cos(\gamma_j + sign(\phi_i - \phi_{cj})\frac{\pi}{4} - \phi_{cj})}{\cos(\gamma_j + sign(\phi_i - \phi_{cj})\frac{\pi}{4} - \phi_i)} \ \ldots\right]^T$$

$$\mathbf{H_j} = \begin{bmatrix} \cdots & \cdots & \cdots \\ \frac{\partial r_i}{\partial \phi_c} & 1 & \frac{\partial r_i}{\partial \gamma} \\ \cdots & \cdots & \cdots \end{bmatrix} \tag{16}$$

$$\mathbf{\Delta b} = (\mathbf{H_j^T H_j})^{-1}\mathbf{H_j^T}(\mathbf{r_m} - \mathbf{r_j}) \tag{17}$$

$$\begin{bmatrix} \phi_{cj+1} \\ r_{cj+1} \\ \gamma_{j+1} \end{bmatrix} = \begin{bmatrix} \phi_{cj} \\ r_{cj} \\ \gamma_j \end{bmatrix} + \mathbf{\Delta b} \tag{18}$$

Equation 17 yields the least squares estimate, and can be found for example in [14]. The advantage of the above mentioned approach is that the corner point is implicitly chosen, and a simple covariance estimate is obtained due to the use of linear regression [22]:

$$cov(\mathbf{\Delta b}) = cov([\phi_c \ r_c \ \gamma]^T) = \sigma_r^2(\mathbf{H^T H})^{-1} \tag{19}$$

As shown in [6], the Sick PLS output is influenced by systematic errors. To gain a worst case systematic error estimate, similarly to [6], contributions from each range error source are calculated using (17) by replacing $(\mathbf{r_m} - \mathbf{r_j})$ with the estimated range systematic errors. The absolute values to systematic errors are then summed up, and their square is added to the diagonal elements of the random error covariance matrix.

The disadvantage of this corner fitting approach is the slight possibility of divergence when the initial choice of

parameters has a large error. To improve robustness, in each iterations we remove those r_{ji} from $\mathbf{r}_j$ which are either negative or they are larger than twice of the measured range r_{mi}.

An example of the corner fitting algorithm is shown in fig. 3 where the convergence from a deliberately poor initial corner estimate is shown. In practice at most 10 iterations are necessary. The computational load is small compared to SLAM in section IV.

Time registration problem

In our experiments we found that there is a significant and varying delay between the time the scan physically commenced and reception of the first bytes of the results. This delay can cause a large error when the robot moves quickly. To account for this we estimate errors for corners and lines using the speed of the robot and a time registration error. The squares of these errors are then added to the diagonals of the corresponding measurement error covariance matrices in the Kalman filter implementation.

III. Sonar and Laser Synergy

The benefits of combining sonar and laser measurements are as follows:

- *Increase in the accuracy of measurements.* The greater the number of measurements fused, usually the more accurate are the results.
- *Enhancement in measurement reliability.* If the same feature is observed by two sensing modalities, the existence of that feature is more likely.
- *More robust laser segmentation.* Due to the limited range and bearing resolution of the laser, measurements from different features can be erroneously segmented into one line segment. However by using sonar observations, the correctness of segmentation can be improved. This can avoid some systematic measurement errors due to incorrect laser associations.
- *Removal of specular reflections.* Using information from laser scans, phantom multiple reflection sonar measurements can be removed more easily compared to using sonar alone.

We have chosen the following scheme for sonar and laser synergy: sonar aids laser segmentation; laser helps to remove spurious sonar measurements and to select good sonar point features. Laser and sonar features of the same object are fused and statistics are kept for each feature as to their sensor type contribution.

While combining laser and sonar measurements, we have assumed that sonar and laser are observing the same features, the speed of sound used in the calculations is reasonably accurate and the robot short term odometry is reasonably accurate.

A. Segmentation

For each laser scan, sonar readings 6 second before and 6 seconds after a laser scan are transformed into the laser coordinate frame using odometry information. This time window is chosen to include one full swipe of each sonar and therefore provide sonar coverage for the whole laser scan.

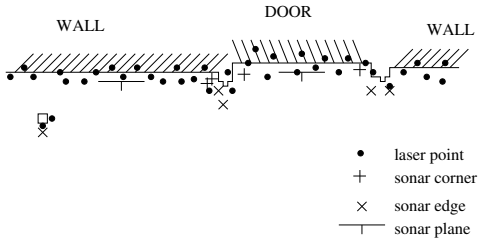

Fig. 4. Laser scan segmentation aided by sonar. Note the sonar measurements are offset from the wall for clarity only.

In the next step sonar readings are clustered. Clusters distant from laser readings are tagged as invisible and are not processed further with this scan.

In the laser segmentation step, each point not already part of a line forms the start of new line segment. The segment grows until any of the following conditions is satisfied:

- There is a discontinuity in the scan.
- The standard deviation of point distances from the line exceeds a set threshold.
- The distance of the next 3 points from the line exceeds a threshold derived from a range error model.
- The range of a point is further than a threshold. This is to stop fitting lines to measurements which are too far from the robot.
- The end of the 180° scan is reached.
- There is a cluster of sonar readings containing corners or edges in the vicinity.

A completed line segment containing more then a set number of points is accepted as a valid line segment and the conditions under which it was completed are stored. The start condition of the next line inherits the terminating condition of the previous line candidate. Line segment end conditions play an important role in our implementation of SLAM.

Sonar clusters containing corners and edges that terminate line segments are good candidates for point features. They are especially good if they are grouped close together, and if they are close to the line. Sonar readings closest to the centers of a such clusters are selected as good point features. Such point features ease association, and reduce the number of features in the map by discarding isolated targets such as chair legs.

In the next phase, extracted laser lines that are separated by a sonar corner are checked if they constitute a right angle corner. If so, a corner is fitted to the raw data points with the approach described in subsection II-C. The number of sonar corners are then stored with the laser corner and vice versa.

Statistics from sonar measurements before clustering are kept on each laser line segment and laser corner to allow confirmation of the existence of features after each 12 second window. At the end of the scan processing, all laser lines, corners and their uncertainties are transformed into

the robots reference frame.

An example for sonar laser segmentation is depicted in fig. 4, where there is a wall, a door and table leg shown as a square. The line growing starts on the righthand side and stops at the right door frame due to sonar edge and corner returns. This line is rejected since it consists of too few line points. A new line is grown between the right and left door frames and is accepted since it contains enough points. The next valid line is grown from the left frame until the table leg where there is a sonar edge and a range discontinuity. Other segmenting methods such as Split and Merge [2] or RANSAC [10] would probably have segmented each scan point except those associated with the table leg as one segment. Our segmentation approach is conservative since it assumes that each line segment belongs to a different object. This assumption reduces the chance of systematic measurement errors in SLAM due to incorrect segmentation. For example let's assume in the map there is a line feature entailing both parts of walls and the door. If an observation contains only part of the door and part of the wall due to obstruction, then there will be a systematic error component in the innovation error.

This segmenting approach can result in a large number of map features, however we do allow line merging as described in the next section and the table leg in fig. 4 will not have a lasting effect on the map.

B. Fusion

A laser line segment or corner having a corresponding sonar line or corner get fused if the sonar readings time stamp is closest to that particular laser scans time stamp. Fusion is done in a Kalman filter fashion, where each measurement is weighted by its uncertainty:

$$\mathbf{z_f} = \mathbf{A}\mathbf{x_l} + \mathbf{B}\mathbf{x_s} \tag{20}$$

where $\mathbf{z_f}$ is the fused measurement, $\mathbf{x_l}$, $\mathbf{C_l}$ is the laser measurement and covariance matrix, $\mathbf{x_s}$, $\mathbf{C_s}$ is the sonar measurement and covariance matrix and

$$\mathbf{A} = \frac{\mathbf{C_l^{-1}}}{\mathbf{C_l^{-1}} + \mathbf{C_s^{-1}}}, \quad \mathbf{B} = \frac{\mathbf{C_s^{-1}}}{\mathbf{C_l^{-1}} + \mathbf{C_s^{-1}}}. \tag{21}$$

The estimated covariance matrix of the fused feature $\mathbf{x_f}$ is calculated as:

$$\mathbf{C_f} = \mathbf{A}\mathbf{C_l}\mathbf{A^T} + \mathbf{B}\mathbf{C_s}\mathbf{B^T} \tag{22}$$

In the case of corners, all computations are done only for the range and bearing, since sonar cannot measure orientation of corners.

IV. SLAM

The SLAM algorithm is implemented in Matlab using a simple extended Kalman filter version similar to that in [5]. For simplicity speed of sound and odometry parameters are not included into the filter and only line segments, corners and point features are used.

In the current implementation all line segment features used either originate from the laser only or are the result of laser and sonar line fusion. This will be extended later to include sonar only features resulting from glass objects for example. In the state vector, line segments are represented by an angle and the distance of the closest point to the origin. Line segment endpoints are stored separately in Cartesian coordinates, and their position is updated at each state update. The line segment endpoints are also changed upon re-observation. The observations endpoints are projected onto the corresponding line feature from the map. Then the line feature end points are:

- moved towards the observation endpoints in a big step if it is likely that the line ends there, e.g. the line is terminated with sonar edges or corners.
- moved towards the observation endpoints in a small step if the observation's endpoint is unreliable, for example due to termination of the line with poor fitting laser points and no sonar information.
- unchanged if measurement endpoint carries no information. For example if measurement endpoint is inside the map line segment, but was terminated because line went beyond the lasers 180° field of view.

Only line segments longer than 70 cm are used in the results.

Corners are represented in the state as an orientation and Cartesian global coordinates. The endpoints of the corners are stored separately to ease association.

Point features, i.e. clusters of sonar edge/corner measurements represented with a measurement in the middle of the cluster, are stored in the state as Cartesian coordinates.

Association is implemented in a simple way using a validation gate. For line segments, the length of overlap is also checked. If there are two possible map feature candidates for a line segment measurement, with the measurement covering at least 40 cm of both candidates, then line segment features are merged.

V. Experimental Results

To test SLAM with advanced sonar and laser, SLAMbot was driven around our lab with a joystick, then out into the corridor. The robot was then driven from one end of the corridor to the other and back to the lab. Odometry, sonar and laser measurements were logged during the more than 150 meters travelled by the robot. During the experiment, half a dozen people walked past the robot, however no changes to the environment occurred such as closing a door.

All calculations were done off-line in Matlab. The resulting 240 feature map is shown in fig 5. Dots on the figure represent corners and points. The robot managed to keep track of its position throughout the whole experiment. However the created map is not error free. At around (15,6), due to a violation of the flat-floor assumption a line was included in the map across the corridor. The corridor is sloped at one place which caused the laser beams to reflect back from the floor.

For comparison we tried to run SLAM with features from the laser only, but the robot accumulated a large enough error in the direction of the corridor to get lost. Even though there are features on the corridor allowing localization in the direction of the corridor, these features

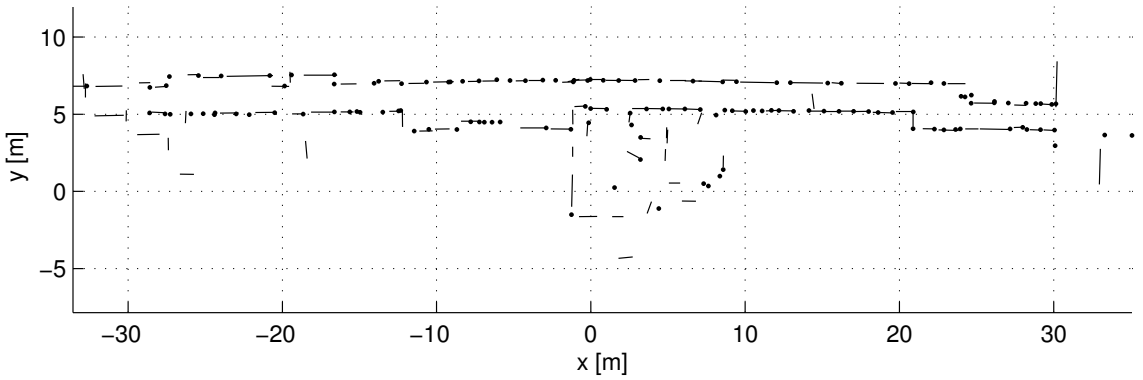

Fig. 5. Slam results on a corridor.

were observed only when the robot was moving in one particular direction due to the 180° field of view of the laser. Therefore the sonar fusion with laser has prevented the divergence of SLAM.

We also ran SLAM using only point landmarks from sonar and the robot kept track of its position.

VI. Conclusion and Future Work

This paper presents our work on performing SLAM using advanced sonar with a laser range finder. This paper also demonstrated successful fusion of lines and corners measured with sonar and laser. The synergistic properties of sonar and laser measurements have been exploited in this work to aid laser line and corner segmentation with advanced sonar readings. Laser measurements, on the other hand can simplify and improve the selection of reliable sonar point features and assist in removing multiple reflection sonar phantom features.

We have also presented a novel right angle corner fitting approach for laser measurements which enables simple error covariance estimation through the minimization of sum of square range residuals.

Future work will compare our maps with a ground truth map generated using a precise laser tracking instrument.

Acknowledgments

The funding of the ARC centre for Perceptive and Intelligent Machines in Complex Environments is acknowledged. Steve Armstrong is gratefully acknowledged for technical support.

References

[1] K. O. Arras. *Feature-Based Robot Navigation in Known and Unknown Environments*. PhD thesis, École Polytechnique Fédérale de Lausanne, 2003.

[2] D. H. Ballard and Brown C. M. *Computer Vision*. Prentice Hall, New Jersey, 1982.

[3] J. A. Castellanos and J. D. Tardós. *Mobile Robot Localization and Map Building, A Multisensor Fusion Approach*. Kluwer Academic Publisher, Norwell, Massachusetts, 1999.

[4] K. S. Chong and L. Kleeman. Feature-based mapping in real, large scale environments using an ultrasonic array. *IJRR*, 18, No. 1:3–19, Jan 1999.

[5] A. Davison. *Mobile Robot Navigation Using Active Vision*. PhD thesis, University of Oxford, 1998.

[6] A. Diosi and L. Kleeman. Uncertainty of line segments extracted from static sick pls laser scans. In *Proceedings of the 2003 Australasian Conference on Robotics and Automation*, 2003.

[7] G. Dudek, P. Freedman, and I. M. Rekleitis. Just–in–time sensing: efficiently combining sonar and laser range data for exploring unknown worlds. In *Proc. of the 1996 IEEE Int. Conf. on Robotics & Automation*, pages 667–671, Minneapolis, Minnesota, April 1996. IEEE.

[8] S. Enderle, G. Kraetzschmar, S. Sablatnög, and G. Palm. Sonar interpretation learned from laser data. In *Proceedings of the Third European Workshop on Advanced Mobile Robots (EUROBOT'99)*, pages 121–126, Zurich, Switzerland, 1999.

[9] H. J. S. Feder, J. J. Leonard, and C. M. Smith. Adaptive mobile robot navigation and mapping. *IJRR*, pages 650–668, July 1999.

[10] M. Fischler and R. Bolles. Random sampling consensus: a paradigm for model fitting with application to image analysis and automated cartography. *Commun. of the ACM*, 24(6):381–395, 1981.

[11] W. Gander and J. Hřebíček. *Solving Problems in Scientific Computing Using Maple and MATLAB*. Springer–Verlag, Berlin, Heidelberg, 1993.

[12] P. Jensfelt. *Approaches to Mobile Robot Localization in Indoor Environments*. PhD thesis, KTH, 2001.

[13] K.-L. Jörg. World modeling for an autonomous mobile robot using heterogenous sensor information. *Robotics and Autonomous Systems*, 14:159–170, 1995.

[14] Steven M. Kay. *Fundamentals of Statistical Signal Processing*, volume 2. Estimation Theory. Prentice Hall, New Jersey, 1993.

[15] K.-H. Kim and H. S. Cho. Range and contour fused environment reckognition for mobile robot. In *Proceedings on International Conference on Multisensor Fusion and Integration for Intelligent Systems*, pages 183–188, Dusseldorf, Germany, Aug. 2001. IEEE.

[16] L. Kleeman. On-the-fly classifying sonar with accurate range and bearing estimation. In *IEEE/RSJ Int. Conf. on Intelligent Robots & Systems*, pages 178–183. IEEE, 2002.

[17] L. Kleeman. Advanced sonar and odometry error modeling for simultaneous localization and map building. In *Proc. of the 2003 IEEE/RSJ Intl. Conf. on Intelligent Robots & Systems*, pages 699–704, Las Vegas, Nevada, October 2003. IEEE.

[18] J. Nieto, J. Guivant, and E. Nebot. Fastslam: Real time implementation in outdoor environments. In *Proc. of the Australasian Conf. on Robotics & Automation*, Auckland, 2002. ARAA.

[19] P. E. Rybski, S. I. Roumeliotis, M. Gini, and N. Papanikolopoulos. Appearance-based minimalistic metric slam. In *Proc. of the 2003 IEEE/RSJ Intl. Conf. on Intelligent Robots & Systems*, pages 194–199, Las Vegas, Nevada, 2003. IEEE.

[20] C. Schlegel and T. Kämpke. Filter design for simultaneous localization and map building (slam). In *Proc. of the 2002 IEEE Int. Conf. on Robotics & Automation*, pages 2737–2741, Washington, DC, May 2002. IEEE.

[21] J. Vandorpe, H. V. Brussel, and H. Xu. Lias: A reflexive navigation architecture for an intelligent mobile robot system. *IEEE Transactions on Industrial Electronics*, 43:432–44, June 1996.

[22] G. B. Wetherill. *Regression analysis with applications*. Chapman and Hall, London, 1986.